

Nuclear magnetic relaxation in an Ising-like antiferromagnet CsCoCl_3 : Domain-wall dynamics

T. Kohmoto

Graduate School of Science and Technology, Kobe University, Nada, Kobe 657, Japan

T. Goto and S. Maegawa

Graduate School of Human and Environmental Studies, Kyoto University, Sakyo-ku, Kyoto 606, Japan

N. Fujiwara

Institute for Solid State Physics, University of Tokyo, Roppongi, Minato-ku, Tokyo 106, Japan

Y. Fukuda

Graduate School of Science and Technology, Kobe University, Nada, Kobe 657, Japan

M. Kunitomo

Department of Physics, Faculty of Science, Kobe University, Nada, Kobe 657, Japan

M. Mekata

Department of Applied Physics, Faculty of Engineering, Fukui University, Bunkyo, Fukui 910, Japan

(Received 26 August 1997)

The longitudinal relaxation time T_1 of ^{133}Cs NMR was measured in the low-temperature, intermediate, and paramagnetic phases of a quasi-one-dimensional $S=1/2$ Ising-like antiferromagnet CsCoCl_3 . The direction and the fluctuating rate of the anisotropic local-field fluctuation at the Cs site, which is caused by passage of domain walls in the Co^{2+} linear chain, are determined by using a fluctuating-field analysis of NMR-line, frequency, and temperature dependences of $1/T_1$. It is found that the fluctuation in the low-temperature phase is of a biaxial pulselike type as a result of temporary spin inversion in the two chains on the triangular lattice, while that in the intermediate phase is of a uniaxial two-state type as a result of the spin inversion only in the disordered chain. The fluctuating rate, ranged over eight orders of magnitude, is obtained from the fluctuating-field analysis. [S0163-1829(98)05805-6]

I. INTRODUCTION

The magnetic linear chain on the triangular lattice is known to show various types of characteristic spin structure and attractive dynamical behavior. The hexagonal compound CsCoCl_3 is a typical example of quasi-one-dimensional $S=1/2$ Ising-like antiferromagnets on the triangular lattice.¹ Much work has been done on this compound experimentally²⁻¹⁹ and theoretically.²⁰⁻²⁹ Especially, much attention has been directed to the spin-frustration effect on the triangular lattice,²¹ which appears as the successive phase transitions at $T_{N1}=21$ K and $T_{N2}=9$ K,³ and the propagation of the domain-wall soliton²⁰ in the intermediate ($T_{N2} < T < T_{N1}$) and the paramagnetic ($T_{N1} < T$) phases. The intermediate phase between T_{N1} and T_{N2} is a partially disordered phase where two-thirds of the magnetic chains order antiferromagnetically with each other leaving the rest uncorrelated. The dynamical behavior in the Ising-like linear chain can be described by the domain-wall picture. The existence of the propagating domain-wall solitons in the Co^{2+} chain in those phases has been established by the neutron-scattering,^{4,6} electron-spin-resonance (ESR),¹⁰⁻¹² nuclear-magnetic-resonance (NMR),¹⁴ and optical¹⁷ experiments.

In the low-temperature phase below T_{N2} , the Co^{2+} spins, which are ordered antiferromagnetically along the c axis,

take a ferrimagnetic structure in the c plane. In a previous paper,³⁰ we showed the presence of domain-wall pairing in the low-temperature phase, and made clear the mechanism of the phase transition at T_{N2} from the dynamic point of view. We also showed the evidence for sublattice switching in the low-temperature phase,³¹ which has much slower dynamics of the order of 10^2 s.

The spins in the linear chain on the triangular lattice show various types of dynamical behavior, and the study of the spin dynamics is very attractive. In the present paper, in order to make the spin dynamics clear in the whole temperature range, the longitudinal relaxation time T_1 of ^{133}Cs NMR was measured in the low-temperature, intermediate, and paramagnetic phases. We pay attention to the NMR-line dependence of $1/T_1$, and analyze the experimental results from the viewpoint of the local-field fluctuation due to the domain-wall passage in the linear chain. The line dependence gives information on the direction of the local fluctuating field, because it is caused by the difference of the angle between the directions of the fluctuating field and the external field, and then the information on the spin dynamics of the individual chain on the triangular lattice can be obtained.

The direction and the fluctuating rate of the anisotropic local-field fluctuation are determined in the low-temperature and the intermediate phases by using a fluctuating-field analysis of NMR-line, frequency, and temperature depen-

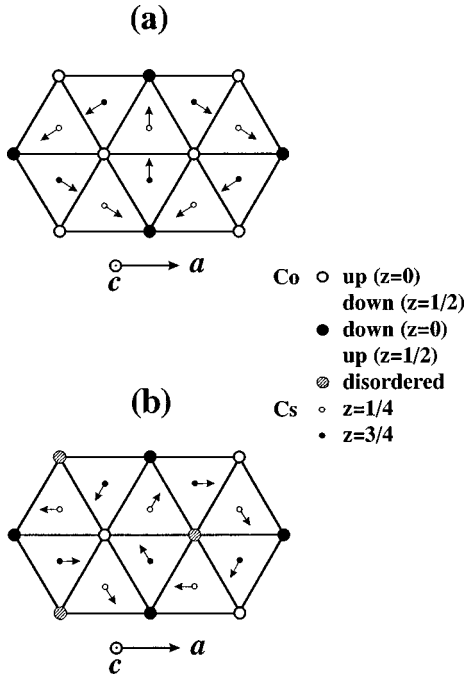


FIG. 1. Spin structure of the Co^{2+} ions and internal field at the Cs nuclei in the c plain (a) in the low-temperature phase and (b) in the intermediate phase.

dences of $1/T_1$. We show that the local-field fluctuation at the Cs nuclei in the low-temperature phase is biaxial and it suggests temporary spin inversion occurs in two of the three chains on the triangular lattice, while that in the intermediate phase is uniaxial and it suggests spin inversion occurs only in the disordered chain. The fluctuating rate of the local field due to the spin inversion, which varies over a wide range of magnitude, is obtained from the fluctuating-field analysis.

II. EXPERIMENT

The hexagonal CsCoCl_3 is one of the typical Ising-like antiferromagnets on the triangular lattice and is known to be a good realization of the magnetic linear chain. Assuming the chain axis to be along the z axis, the intrachain Hamiltonian is given by

$$\mathcal{H} = -2J \sum_j \{S_j^x S_{j+1}^x + \varepsilon (S_j^x S_{j+1}^y + S_j^y S_{j+1}^y)\}, \quad (1)$$

where $S = 1/2$, $J = -75$ K, and $\varepsilon \approx 0.14$.²⁴ The nearest-neighbor interchain interaction J_1 is antiferromagnetic and is much weaker than the intrachain interaction ($J_1/J \sim 10^{-2}$).²²

In the low-temperature phase, the electron spins of the Co^{2+} ions in all the linear chains are ordered antiferromagnetically, and the Co^{2+} chains on the triangular lattice take a collinear ferrimagnetic arrangement in the c plane as shown in Fig. 1(a). In the intermediate phase, on the other hand, one-third of the chains are disordered as shown in Fig. 1(b). The domain-wall solitons propagate in the disordered chain.

The Cs nucleus is located in the center of the six Co^{2+} ions which form a triangular prism with a threefold axis along the c axis. The dipolar interactions with the surrounding Co^{2+} magnetic moments give rise to the internal field \mathbf{h}_0 at the Cs nucleus, whose direction lies in the c plane.¹³ Both

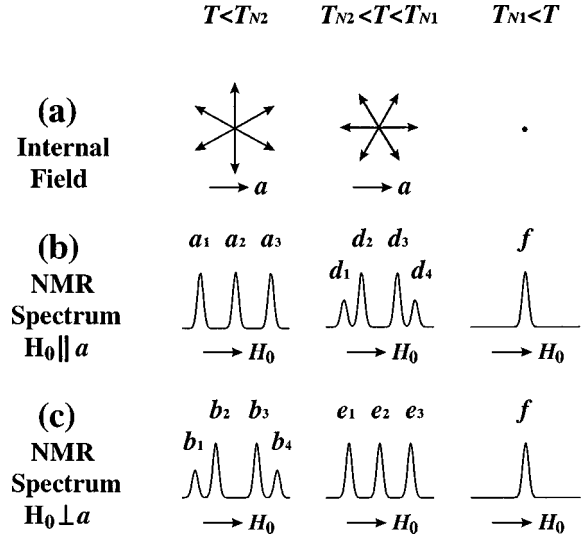


FIG. 2. (a) Six directions of the internal fields in the c plain at the six Cs sites, (b) schematic NMR spectra observed in $\mathbf{H}_0 \parallel \mathbf{a}$ axis, and (c) schematic NMR spectra observed in $\mathbf{H}_0 \perp \mathbf{a}$ axis in the low-temperature ($T < T_{N2}$), the intermediate ($T_{N2} < T < T_{N1}$), and the paramagnetic ($T_{N1} < T$) phases.

in the low-temperature and the intermediate phases, there are six magnetically nonequivalent Cs sites where the directions of the internal field are different in the c plane as is seen in Fig. 2(a), although the directions and the magnitude of the internal field are different between the two phases. For the low-temperature phase, three of the directions are shown by the arrows in Fig. 1(a), while the others appear in other domains in the c plane.

In the presence of an external field \mathbf{H}_0 , the total magnetic field at each Cs site is determined by the vector sum of \mathbf{H}_0

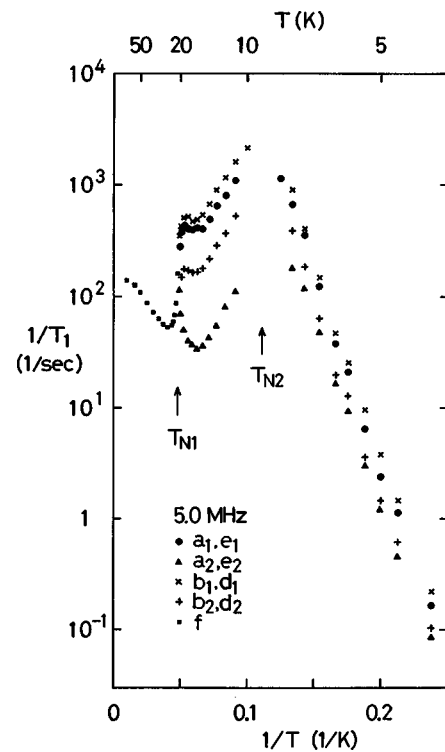


FIG. 3. Temperature dependences of $1/T_1$ at $\omega/2\pi = 5.0$ MHz for the temperature range between 4.2 and 100 K.

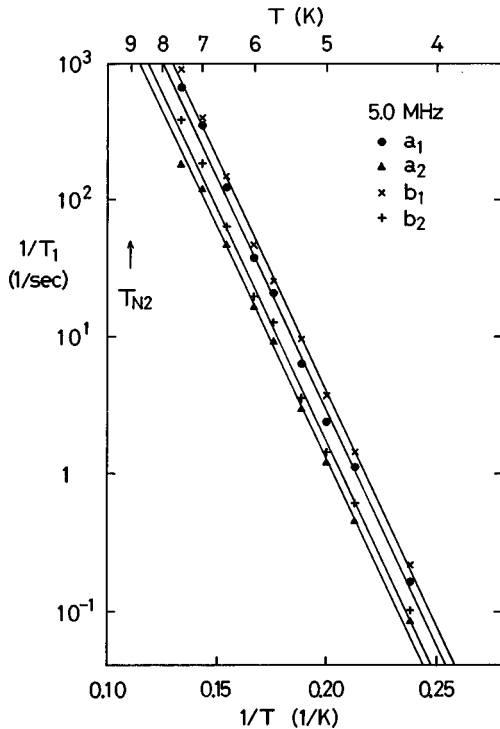


FIG. 4. Temperature dependences of $1/T_1$ at $\omega/2\pi = 5.0$ MHz for the a_1 , a_2 , b_1 , and b_2 lines in the low-temperature phase. The values of $1/T_1$ for the a_3 , b_3 , and b_4 lines are the same as those for the a_1 , b_2 , and b_1 lines, respectively, within the experimental error. The solid lines represent the fitting lines obtained from the relation $1/T_1 \propto \exp(-|J|/kT)$.

and \mathbf{h}_0 . When the external field is applied in the c plane and its magnitude is swept with the operating frequency fixed, six NMR lines at most can appear corresponding to the different directions of the internal field. In the case of the low-temperature phase, three NMR lines, which we refer to as a_1 – a_3 lines, appear in the external field parallel to the a axis as shown in Fig. 2(b), and four lines, which we refer to as b_1 – b_4 lines, appear in the external field perpendicular to the a axis as shown in Fig. 2(c). In the case of the intermediate phase, four lines (d_1 – d_4) appear in the field parallel to the a axis, and three lines (e_1 – e_3) appear in the field perpendicular to the a axis. In the paramagnetic phase, a single line (f) appears for any direction of the external field. The values of T_1 were measured for these 15 lines.

The experiment was made by using a coherent pulsed-NMR spectrometer equipped with a personal computer for the pulse-sequence control and the signal processing. The longitudinal relaxation time T_1 was measured at the resonance frequency $\omega/2\pi = 1.5$ – 6.7 MHz ($H_0 = 2$ – 12 kOe) in the temperature range between 4.2 and 100 K. The value of T_1 was determined by observing the recovery of the spin-echo signal after the saturation by a comb of rf pulses.

III. EXPERIMENTAL RESULTS

The temperature dependences of $1/T_1$ at $\omega/2\pi = 5.0$ MHz for the whole temperature range are shown in Fig. 3. Those for the low-temperature phase and those for the intermediate and paramagnetic phases are shown in Figs. 4 and 5, respectively. Near the temperature T_{N2} , the measurement of

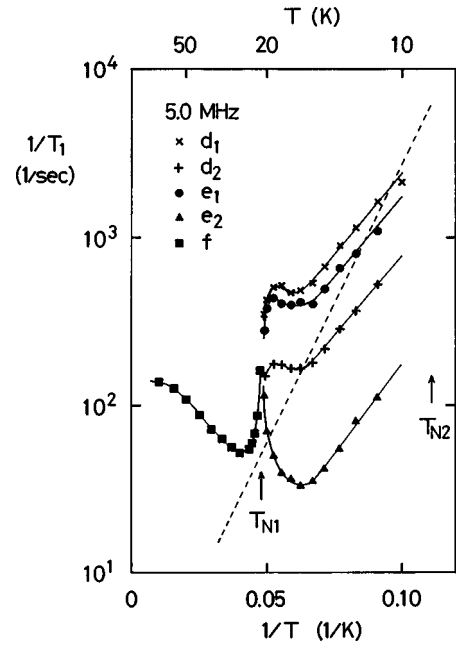


FIG. 5. Temperature dependences of $1/T_1$ at $\omega/2\pi = 5.0$ MHz for the d_1 , d_2 , e_1 , and e_2 lines in the intermediate phase and the f line in the paramagnetic phase. The values of $1/T_1$ for the d_3 , d_4 , and e_3 lines are the same as those for the d_2 , d_1 , and e_1 lines, respectively, within the experimental error. The solid lines are guide for the eyes. The broken line shows the slope expected from the relation $1/T_1 \propto \exp(|J|/kT)$.

T_1 values was not easy because the transverse relaxation time T_2 becomes very short and the signal intensity of the spin echoes becomes very small.

Figure 4 shows the temperature dependences of $1/T_1$ for the a_1 , a_2 , b_1 , and b_2 lines in the low-temperature phase. The values of $1/T_1$ for the a_3 , b_3 , and b_4 lines are the same as those for the a_1 , b_2 , and b_1 lines, respectively, within the experimental error. The value of $1/T_1$ exhibits a remarkable increase with increasing temperature, and the temperature dependence is well described by the relation $1/T_1 \propto \exp(-|J|/kT)$ for all lines and frequencies.³⁰ The solid lines in Fig. 4 represent the fitting lines obtained from the above relation.

Figure 5 shows the temperature dependences of $1/T_1$ for the d_1 , d_2 , e_1 , and e_2 lines in the intermediate phase and the f line in the paramagnetic phase. The values of $1/T_1$ for the d_3 , d_4 , and e_3 lines are the same as those for the d_2 , d_1 , and e_1 lines, respectively, within the experimental error. In the intermediate phase the value of $1/T_1$ varies over one order of magnitude depending on the line, and with increasing temperature the values for all lines become the same at the temperature T_{N1} . The large line dependence in the intermediate phase is different from that in the case of the low-temperature phase. According to the model of the propagating domain-wall solitons in the disordered chains, the temperature dependence in the intermediate phase is expected as $1/T_1 \propto \exp(|J|/kT)$.¹⁴ The broken line in Fig. 5 shows the expected slope. The slope obtained from the experimental data is smaller than the expected one.

The angular dependences of $1/T_1$ at the temperature $T = 5.7$ K and at the frequency $\omega/2\pi = 2.0$, 3.0, 5.0, and 6.7 MHz are shown in Fig. 6. The seven data for a fixed fre-

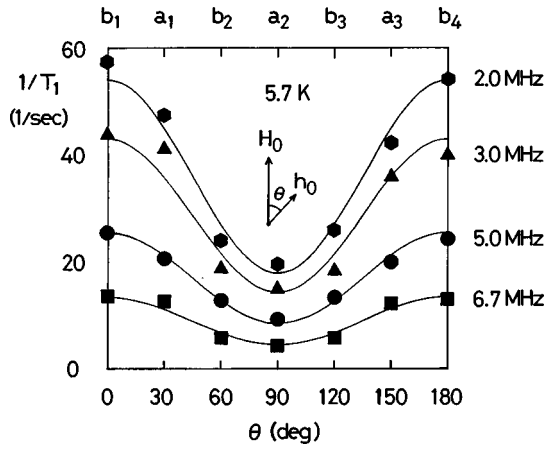


FIG. 6. Angular dependences of $1/T_1$ at the temperature $T = 5.7$ K and at the frequency $\omega/2\pi = 2.0, 3.0, 5.0,$ and 6.7 MHz. θ represents the angle between the directions of the external field \mathbf{H}_0 and the internal field \mathbf{h}_0 at the Cs site. The seven data for a fixed frequency are the measured values of $1/T_1$ for the seven NMR lines, the a_1 – a_3 lines in Fig. 2(b) and the b_1 – b_4 lines in Fig. 2(c). The solid lines represent the theoretical curve obtained from the best fit of Eq. (5) to the measured values.

quency are the measured values of $1/T_1$ for the seven NMR lines, the a_1 – a_3 lines in Fig. 2(b), and the b_1 – b_4 lines in Fig. 2(c). Here θ represents the angle between the directions of the external field \mathbf{H}_0 and the internal field \mathbf{h}_0 at the Cs site. Since $H_0 \gg h_0$ in our experimental condition, $|\mathbf{H}_0 + \mathbf{h}_0| \approx H_0 + h_0 \cos \theta$. The values of θ corresponding to the $a_1, a_2, a_3, b_1, b_2, b_3,$ and b_4 lines are $30^\circ, 90^\circ, 150^\circ, 0^\circ, 60^\circ, 120^\circ,$ and 180° , respectively. Similar angular and frequency dependences were observed at the other temperatures in the low-temperature phase,³⁰ although the value of $1/T_1$ exhibited remarkable temperature dependence.

The angular dependence of $1/T_1$ at the temperature $T = 15$ K and at the frequency $\omega/2\pi = 5.0$ MHz is shown in Fig. 7. The seven data are the measured values of $1/T_1$ for the

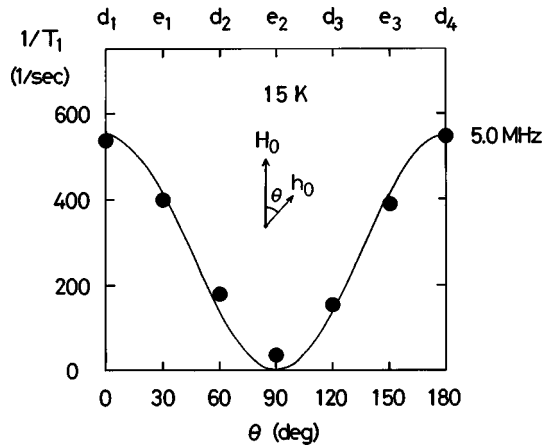


FIG. 7. Angular dependence of $1/T_1$ at the temperature $T = 15$ K and at the frequency $\omega/2\pi = 5.0$ MHz. θ represents the angle between the directions of the external field \mathbf{H}_0 and the internal field \mathbf{h}_0 at the Cs site. The seven data are the measured values of $1/T_1$ for the seven NMR lines, the d_1 – d_4 lines in Fig. 2(b) and the e_1 – e_3 lines in Fig. 2(c). The solid line represents the theoretical curve obtained from the best fit of Eq. (8) to the measured values.

seven NMR lines, the d_1 – d_4 lines in Fig. 2(b), and the e_1 – e_3 lines in Fig. 2(c). The values of θ corresponding to the $d_1, d_2, d_3, d_4, e_1, e_2,$ and e_3 lines are $0^\circ, 60^\circ, 120^\circ, 180^\circ, 30^\circ, 90^\circ,$ and 150° , respectively. The value of $1/T_1$ in the intermediate phase did not exhibit appreciable frequency dependence; the value of T_1 of each line for different frequencies was the same in our frequency range within experimental error.

As is seen in Figs. 6 and 7, the longitudinal relaxation rates in the low-temperature and the intermediate phases exhibit characteristic angular (θ) dependences, respectively. The value of $1/T_1$ takes the minimum value for $\theta = 90^\circ$ and the maximum value for $\theta = 0^\circ$ and 180° in both phases. In the low-temperature phase the former is about one-third of the latter, while in the intermediate phase the former is smaller than one-tenth of the latter. This suggests that the fluctuation at the Cs site is biaxial in the low-temperature phase and is uniaxial in the intermediate phase. It is interesting that the $1/T_1$ in the low-temperature phase depends on the NMR frequency ω but that in the intermediate phase does not. This suggests that the characteristic time of the local-field fluctuation is longer than $1/\omega$ in the low-temperature phase and is shorter in the intermediate phase.

IV. DISCUSSION

In order to explain the characteristic angular and frequency dependences and those differences between the intermediate and the low-temperature phases, we consider an analysis of the fluctuating internal field at the Cs nuclei.

According to the conventional stochastic theory of relaxation,^{32,33} the relaxation rate is described by using the time-correlation function for the fluctuating field. The longitudinal relaxation rate $1/T_1$ is given by

$$\frac{1}{T_1} = \frac{\gamma^2}{2} \int_{-\infty}^{+\infty} \langle \delta h_{\perp}(t) \delta h_{\perp}(0) \rangle \exp(i\omega t) dt, \quad (2)$$

where γ is the gyromagnetic ratio, and $\delta h_{\perp}(t)$ represents the transverse components of the fluctuating local field. If we assume an exponential type of correlation function,

$$\langle \delta h_{\perp}(t) \delta h_{\perp}(0) \rangle = \Delta^2 \exp(-|t|/\tau_c), \quad (3)$$

where $\Delta^2 = \langle (\delta h_{\perp})^2 \rangle$, and τ_c is the correlation time of the fluctuating field, then the expression of $1/T_1$ can be calculated easily from Eqs. (2) and (3);

$$\frac{1}{T_1} = (\gamma\Delta)^2 \frac{\tau_c}{1 + (\omega\tau_c)^2}. \quad (4)$$

The relaxation rate is determined by the amplitude Δ and the correlation time τ_c of the fluctuation.

As is seen in Eq. (4), the characteristic of the frequency dependence of $1/T_1$ is determined by the value of $\omega\tau_c$. In the case of $\omega\tau_c \gg 1$, the longitudinal relaxation rate is proportional to $1/\omega^2$. In the case of $\omega\tau_c \ll 1$, on the other hand, the rate is independent of ω . The longitudinal relaxation in the intermediate phase, which was independent of the NMR frequency, corresponds to the latter case where the correlation time is shorter than $1/\omega$.

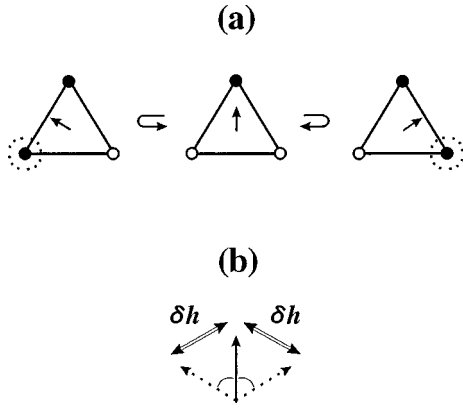


FIG. 8. (a) Temporary rotation of the internal field and (b) biaxial fluctuation in the c plane at the Cs site in the low-temperature phase when the spin inversion occurs in one of the Co^{2+} chains on the triangular lattice.

Here, to explain the experimental results, we pay attention to the local-field fluctuation due to the spin inversion in the linear chain which is caused by the passage of domain walls. As for the case of the low-temperature phase, we have discussed the possibility of domain-wall pairing in the linear chain by using an analysis of the fluctuating internal field in the previous paper.³⁰ In the following, we summarize the result of the analysis to compare with the case of the intermediate phase.

We considered a temporary spin-inversion model; the Co^{2+} spins are inverted locally in the linear chain for a short time away from the stable directions which are determined by the ferrimagnetic structure in the c plane. It is expected that the spin inversion may occur in either of the two [open circles in Fig. 1(a)] of the three chains on the triangular lattice. If the spin inversion occurs in one linear chain, the direction of the internal field rotates by $\pm 60^\circ$ in the c plane as shown in Fig. 8. The fluctuating field at the Cs nucleus due to the spin inversion is a pulselike fluctuation as shown in Fig. 10(a). The component $\delta h_\perp(t)$ of the field fluctuation jumps back and forth between the stable direction with lifetime τ_0 and the unstable direction with averaged pulse area $h_\perp \tau_1$. We assume $\tau_0 \gg \tau_1$, since the direction of the internal field is stable in the three-dimensionally ordered phase. Each pulse has a temporal structure of the order of τ_c .

There are two kinds of pulselike fluctuations whose field jumps are h_\perp^\pm corresponding to the $\pm 60^\circ$ rotations. The relaxation rate is given by the sum of these two contributions;

$$\frac{1}{T_1} = \frac{\tau_1}{\tau_0} \frac{\gamma^2}{4} \{ (h_\perp^+)^2 + (h_\perp^-)^2 \} \frac{\tau_c}{1 + (\omega \tau_c)^2}, \quad (5)$$

where $1/\tau_0$ is the fluctuation pulse rate at the Cs site, and then the spin-inversion rate in each of the two Co^{2+} chains is $1/2\tau_0$. The θ dependence of the fluctuating field is given by

$$h_\perp^\pm = h_0 \{ \sin(\theta \pm 60^\circ) - \sin\theta \}. \quad (6)$$

In the case of the low-temperature phase, the fluctuation at the Cs site is not uniaxial but biaxial as shown in Fig. 8(b).

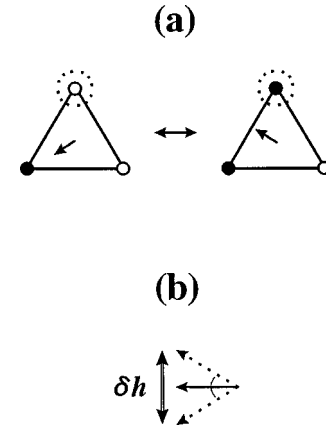


FIG. 9. (a) Switching of the internal field and (b) uniaxial fluctuation in the c plane at the Cs site in the intermediate phase when a domain wall passes in the disordered chain.

The angular dependence of $1/T_1$ is determined by $(h_\perp^+)^2 + (h_\perp^-)^2$. The solid lines shown in Fig. 6 represent the theoretical angular dependence obtained from the best fit of Eq. (5) with Eq. (6) to the measured values of $1/T_1$. As is seen, the theoretical curves, which are calculated from the biaxial fluctuation in the above model, explain well the experimental result.

By using Eqs. (5), (6), and the experimentally evaluated values $\tau_c \approx 4 \times 10^{-8}$ s and $\tau_1 \approx 1.6 \times 10^{-6}$ s,³⁰ we can determine the value of τ_0 from the observed values of $1/T_1$. Temperature dependence of the fluctuation pulse rate $1/\tau_0$ of the internal field at the Cs site is shown in Fig. 11.

The spin dynamics in the Co^{2+} chain deduced from the pulselike fluctuation at the Cs site is as follows. The Co^{2+} spins, which lies in the ferrimagnetic stable directions, are inverted locally in the chain for a short time. The magnetic excitation is created thermally at the rate of $1/\tau_0$, and the rate increases exponentially as the temperature is increased. The magnetic excitation moves back and forth in the linear chain with a characteristic time τ_c and is annihilated spontaneously with a lifetime of the order of τ_1 . This interpretation suggests domain-wall pairing in the Co^{2+} chain.

Now we consider the case of the intermediate phase. In this case, domain-wall solitons propagate in one of the three chains. The spin inversion caused by the passage of the domain wall changes the internal field at the Cs site. The direction of the internal field due to the disordered chain is switched rapidly in the c plane. Then the mean field, which is due to the two ordered chains, is parallel to the a axis as shown in Fig. 1(b). In the short-time scale, however, the direction of the vector sum of the internal field rotates by 60° in the c plain as shown in Fig. 9, when a domain wall passes in the disordered chain. The direction of the fluctuating field is perpendicular to the a axis, and its magnitude is $2h_0/\sqrt{3}$, where h_0 is the mean internal field at the Cs site and its value is 0.35 kOe in the intermediate phase from the observed splitting of the NMR spectrum.

The longitudinal relaxation is determined by the transverse component $\delta h_\perp(t)$ of the fluctuating field. In the present case, $\delta h_\perp(t)$ is considered to be a two-state type of fluctuation as shown in Fig. 10(b), and is described by random jumps between two field values with the magnitude h_\perp

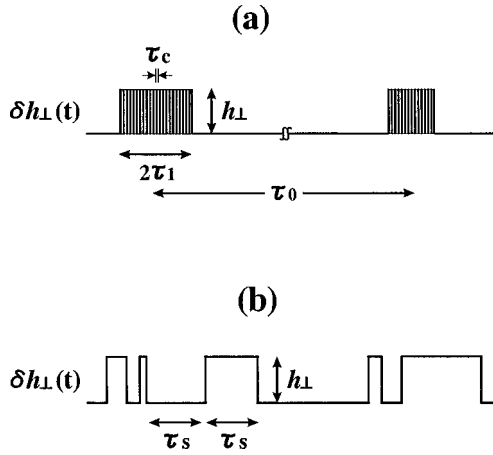


FIG. 10. Transverse component $\delta h_{\perp}(t)$ of the fluctuating field at the Cs site. (a) Pulselike fluctuation in the low-temperature phase with pulse rate $1/\tau_0$, averaged pulse area $h_{\perp}\tau_1$, and a temporal structure of the order of τ_c in a pulse. (b) Two-state fluctuation in the intermediate phase with lifetime τ_s of each state.

of the field jump and the lifetime τ_s of each state. The switching rate of the internal field at the Cs site is $1/\tau_s$, which is also the spin-inversion rate in the disordered chain. The transverse component h_{\perp} of the field jump depends on the NMR line and determined by the angle between the external field \mathbf{H}_0 and the fluctuating field which is perpendicular to the internal field \mathbf{h}_0 ;

$$h_{\perp} = \frac{2}{\sqrt{3}} h_0 \cos\theta, \quad (7)$$

where θ is the same as that in Fig. 7.

The correlation function of the two-state fluctuation can be calculated analytically and expressed by an exponential-type function.³⁴ In the case of Fig. 10(b), the amplitude and the correlation time in Eqs. (3) and (4) are given by $\Delta = h_{\perp}/2$ and $\tau_c = \tau_s/2$. The relaxation rate due to the two-state fluctuation is obtained from Eq. (4);

$$\frac{1}{T_1} = \frac{1}{4} (\gamma h_{\perp})^2 \frac{\tau_s/2}{1 + (\omega\tau_s/2)^2} \approx \frac{1}{8} (\gamma h_{\perp})^2 \tau_s, \quad \omega\tau_s \ll 1. \quad (8)$$

The angular dependence of $1/T_1$ is determined by the square $(h_{\perp})^2$ of the magnitude of the field jump. The solid line shown in Fig. 7 represents the theoretical angular dependence obtained from the best fit of Eq. (8) with Eq. (7) to the measured values of $1/T_1$. As is seen, the theoretical curve, which is calculated from the uniaxial fluctuation in the above model, explains well the experimental result. When the direction of the external field \mathbf{H}_0 is perpendicular to that of the fluctuation ($\theta = 0^\circ$ and 180°), the transverse component is maximum and the value of $1/T_1$ is maximum. When the direction of \mathbf{H}_0 is parallel to that of the fluctuation ($\theta = 90^\circ$), on the other hand, the transverse component is minimum and the value of $1/T_1$ is minimum ($1/T_1 = 0$ in an ideal case).

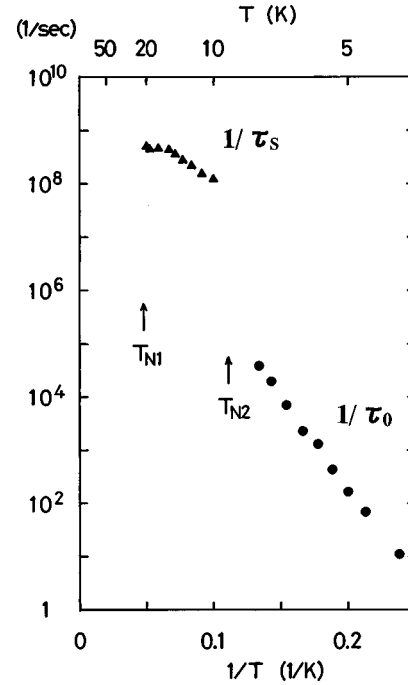


FIG. 11. Temperature dependence of the fluctuating rate of the local field at the Cs site. Fluctuation pulse rate $1/\tau_0$ in the low-temperature phase and switching rate $1/\tau_s$ in the intermediate phase are obtained from the T_1 analysis.

Temperature dependence of the switching rate $1/\tau_s$ of the internal field at the Cs site is shown in Fig. 11. The value of $1/\tau_s$ can be calculated from different lines, which have different values of θ , by using Eqs. (7) and (8). Plotted data in Fig. 11 are averaged values of $1/\tau_s$ calculated from the observed values of $1/T_1$ of the d_1 , d_2 , and e_1 lines in Fig. 5. The values of $1/\tau_s$ obtained from these lines were consistent with each other. As is expected from the frequency independence, the values of $\omega\tau_s$ are much smaller than unity.

The slope of the temperature dependence in Fig. 5 is smaller than that expected from the model of free soliton propagation. It may be possible that a bound state^{9,26,28} of two solitons decreases the activation energy. As for the observed slope in the intermediate phase, however, we do not have a good explanation at the present.

As is shown in Fig. 11, the fluctuating rate due to the movement of the domain walls is obtained in a wide dynamic range of eight orders of magnitude in our experiment, although the meaning of the fluctuating rate is different between the low-temperature phase (the fluctuation pulse rate $1/\tau_0$) and the intermediate phase (the switching rate $1/\tau_s$).

V. SUMMARY

We measured the longitudinal relaxation time T_1 of ^{133}Cs NMR in CsCoCl_3 . The relaxation rate $1/T_1$ exhibits characteristic angular and temperature dependences in the low-temperature and the intermediate phases, respectively. The relaxation rate exhibits NMR-frequency dependence in the low-temperature phase, while does not in the intermediate phase.

From an analysis of fluctuating internal field at the Cs

nuclei, the experimental results were interpreted in terms of a biaxial pulselike fluctuation in the low-temperature phase and a uniaxial two-state fluctuation in the intermediate phase. This interpretation suggests domain-wall pairing in two of the three Co^{2+} chains in the low-temperature phase and domain-wall soliton propagation in one of those in the inter-

mediate phase. The fluctuating rate of the local field caused by the passage of the domain wall, which was evaluated as the fluctuation pulse rate or the switching rate of the local field at the Cs site due to the spin inversion in the Co^{2+} chains, was obtained in a wide range over eight orders of magnitude.

-
- ¹N. Achiwa, *J. Phys. Soc. Jpn.* **27**, 561 (1969).
²U. Tellenbach and H. Arend, *J. Phys. C* **10**, 1311 (1977).
³H. Yoshizawa and K. Hirakawa, *J. Phys. Soc. Jpn.* **46**, 448 (1979).
⁴H. Yoshizawa, K. Hirakawa, S. K. Satija, and G. Shirane, *Phys. Rev. B* **23**, 2298 (1981).
⁵S. E. Nagler, W. J. L. Buyers, R. L. Armstrong, and B. Briat, *Phys. Rev. B* **27**, 1784 (1983).
⁶J. P. Boucher, L. P. Regnault, J. Rossat-Mignod, Y. Henry, J. Bouillot, and W. G. Stirling, *Phys. Rev. B* **31**, 3015 (1985).
⁷T. Nguyen, S. E. Nagler, R. A. Cowley, T. Perring, and R. Osborn, *J. Phys.: Condens. Matter* **7**, 2917 (1995).
⁸J. P. Goff, D. A. Tennant, and S. E. Nagler, *Phys. Rev. B* **52**, 15 992 (1995).
⁹I. Bose and A. Ghosh, *J. Phys.: Condens. Matter* **8**, 351 (1996).
¹⁰K. Adachi, *J. Phys. Soc. Jpn.* **50**, 3904 (1981).
¹¹J. P. Boucher, G. Rius, and Y. Henry, *Europhys. Lett.* **4**, 1073 (1987).
¹²H. Kikuchi and Y. Ajiro, *J. Phys. Soc. Jpn.* **58**, 2531 (1989).
¹³K. Adachi, M. Hamashima, Y. Ajiro, and M. Mekata, *J. Phys. Soc. Jpn.* **47**, 780 (1979).
¹⁴Y. Ajiro, H. Kikuchi, T. Okita, M. Chiba, K. Adachi, M. Mekata, and T. Goto, *J. Phys. Soc. Jpn.* **58**, 390 (1989).
¹⁵H. Kikuchi and Y. Ajiro, *J. Phys. Soc. Jpn.* **58**, 692 (1989).
¹⁶W. P. Lehmann, W. Breitling, and R. Weber, *J. Phys. C* **14**, 4655 (1981).
¹⁷I. Mogi, N. Kojima, Y. Ajiro, H. Kikuchi, T. Ban, and I. Tsujikawa, *J. Phys. Soc. Jpn.* **56**, 4592 (1987).
¹⁸I. Mogi, M. Takeda, G. Kido, Y. Nakagawa, H. Kikuchi, and Y. Ajiro, *J. Phys. Soc. Jpn.* **58**, 2188 (1989).
¹⁹K. Amaya, H. Hori, I. Shiozaki, M. Date, M. Ishizuka, T. Sakakibara, T. Goto, N. Miura, H. Kikuchi, and Y. Ajiro, *J. Phys. Soc. Jpn.* **59**, 1810 (1990).
²⁰J. Villain, *Physica B&C* **79B**, 1 (1975).
²¹M. Mekata, *J. Phys. Soc. Jpn.* **42**, 76 (1977).
²²H. Shiba, *Prog. Theor. Phys.* **64**, 466 (1980).
²³K. Maki, *Phys. Rev. B* **24**, 335 (1981).
²⁴F. Matsubara and S. Ikeda, *Phys. Rev. B* **28**, 4064 (1983).
²⁵M. L. Plumer, A. Caille, and K. Hood, *Phys. Rev. B* **40**, 4958 (1989).
²⁶F. Matsubara and S. Inawashiro, *J. Phys. Soc. Jpn.* **58**, 4284 (1989).
²⁷F. Matsubara and S. Inawashiro, *Phys. Rev. B* **41**, 2284 (1990).
²⁸F. Matsubara and S. Inawashiro, *Phys. Rev. B* **43**, 796 (1991).
²⁹A. Bunker, B. D. Gaulin, and C. Kallin, *Phys. Rev. B* **48**, 15 861 (1993).
³⁰T. Kohmoto, T. Goto, S. Maegawa, N. Fujiwara, Y. Fukuda, M. Kunitomo, and M. Mekata, *Phys. Rev. B* **49**, 6028 (1994).
³¹T. Kohmoto, T. Goto, S. Maegawa, N. Fujiwara, Y. Fukuda, M. Kunitomo, and M. Mekata, *Phys. Rev. B* **52**, 12 526 (1995).
³²R. Kubo, M. Toda, and N. Hashitsume, *Statistical Physics II Non-equilibrium Statistical Mechanics* (Springer-Verlag, Berlin, 1991), p. 40.
³³C. P. Slichter, *Principles of Magnetic Resonance* (Springer-Verlag, Berlin, 1989), p. 206.
³⁴C. P. Slichter, *Principles of Magnetic Resonance* (Springer-Verlag, Berlin, 1989), p. 584.